Electrochemistry Communications 111 (2020) 106650

Contents lists available at ScienceDirect

Electrochemistry Communications

journal homepage: www.elsevier.com/locate/elecom

The role of electrode orientation to enhance mass transport in redox flow batteries

Noemí Aguiló-Aguayo*, Thomas Drozdzik, Thomas Bechtold

Research Institute of Textile Chemistry and Textile Physics, University of Innsbruck, Hoechsterstrasse 73, 6850 Dornbirn, Austria

ARTICLE INFO

Keywords:
Redox flow batteries
Mass transfer coefficient
Electrolyte velocity
Electrodes
Fiber orientation

ABSTRACT

Mass transport plays a crucial role in the performance of redox flow batteries (RFBs). Generally, the electrodes used in RFBs are assemblies of randomly oriented carbon fibers (e.g. graphite felts, carbon papers). It has been shown that ordered arrangements exhibit enhanced mass transport performance (e.g. carbon cloths). Our investigations are focused on evaluating the role of the electrode orientation alone, on the mass transport with electrodes oriented parallel and perpendicular to the electrolyte flow direction. The electrodes employed were prepared with embroidery, and composed of Cu wires 80 μm in diameter. The space between wires was maintained at 1.1 mm during construction to enable complete electrolyte accessibility through the electrode, and the cell structure was designed to ensure uniform electrolyte velocity across the whole electrode surface area. The limiting currents were measured for both electrode orientations with linear sweep voltammetry. The results showed 18% greater mass transport coefficient for the perpendicular orientation as a consequence of greater accessibility of the reactants to the electrode surface. The findings provide insights for the optimization of electrode designs in mass-transport-limited reactors, such as RFBs.

1. Introduction

Electrolyte velocity plays a crucial role when redox reactions occur at an electrode-electrolyte interface and are mass-transfer controlled. This is the case for redox flow batteries (RFBs), where reactants and products are in a solution state (electrolytes) and circulate through a cell where redox reactions occur at the interface with electrodes. Therefore, the maximum power density attained in RFBs, once the ohmic and charge-transfer resistances are minimized, is limited by the mass transport of the electrolytes within the cell [1].

Carbon paper and graphite felts are the most common electrode materials used in RFBs, because of their corrosion resistance, high permeability, and high specific surface areas [2]. These electrodes are composed of a random assembly of carbon fibers, which impedes mass transport of electrolyte within the electrodes. A method of improving this aspect is to insert flow frames next to the electrodes, thus forcing the electrolyte to penetrate through the porous electrodes [3]. Different flow patterns can be achieved, and the most common flow channel architectures are serpentine, interdigitated, parallel and spiral. All other factors being the same, the battery performance changes with the architecture [4,5]. The electrode thickness also has an impact on the electrolyte velocity, and thus on the mass transport in porous electrodes. Numerical simulations revealed that increasing Reynolds number and decreasing electrode thickness have a positive effect on mass transport in porous electrodes in a flow-by configuration [6]. The flow channel architecture and electrode thickness influence the magnitude and uniformity of the electrolyte velocity and the accessibility of electrolyte within the electrodes. The greater these values are, the better the performance. A correlation between the mass transfer coefficient and electrolyte velocity for carbon-felt electrodes in a flow-through configuration was proposed by Qiang Ye and co-authors [7,8]. Mass transfer rates for different flow fields using carbon paper electrodes were also quantified by Brushett et al. [9]. However, there are few studies concerning oriented-fiber electrodes. Numerical simulations of mass transfer in commercially available electrode materials with an anisotropic microstructure revealed that an increase in the electrode permeability caused a decrease in the mass transfer coefficient [10].

Recently, some research has been focused on electrodes with oriented assemblies of carbon fibers, such as carbon cloths. Zhou et al. observed a superior performance with these woven structures, and attributed it to a greater hydraulic permeability, larger pore sizes and lower tortuosity [11,12]. Forner-Cuenca et al. also found higher current densities and lower pressure drops with cloth electrodes, and attributed that to their “periodic, well-defined microstructure” [13]. A common observation is that ordered fiber arrangements exert a positive influence on battery performance.

* Corresponding author.
E-mail addresses: noemi.aguilo-aguayo@uibk.ac.at, textilchemie@uibk.ac.at (N. Aguiló-Aguayo).

https://doi.org/10.1016/j.elecom.2019.106650
Received 29 November 2019; Received in revised form 20 December 2019; Accepted 23 December 2019
Available online 28 December 2019

Even carbon cloths exhibit complexities of fiber orientations as they are twisted into yarns and of electrolyte velocity distributions within the twisted yarns and thus it is difficult to predict the individual influence of each electrode parameter, such as the fiber orientation, porosity, tortuosity, and electroactive surface area.

The motivation of our work was to investigate what influence the fiber orientation alone, isolated from all other possible electrode parameters, exerts on mass transfer coefficients in flow cells. For this purpose, well-defined electrodes were prepared from copper wires with embroidery, and two different electrode orientations were evaluated in a flow-by, half-cell configuration,

(i) an embroidered Cu electrode with wires parallel to the flow direction, and
(ii) an embroidered Cu electrode with wires perpendicular to the flow direction.

3D-printing was employed to create a flow distributor frame to provide a uniform flow across the electrode surface. The electrolyte used in these experiments was iron(III)-triethanolamine (Fe(III)-TEA) in alkaline medium. Linear sweep voltammetry curves were evaluated at different electrolyte velocities. Limiting current densities at multiple electrolyte volumetric flow rates were measured, and the dependence of the mass transfer coefficient with electrolyte velocity was calculated. The findings provide some insights for the optimization of electrodes in redox flow batteries.

2. Materials and methods

Fig. 1a shows the constructed cell. An acrylonitrile butadiene styrene (ABS) 3D-printed frame was used as a flow-distributor, and placed between two extruded polycarbonate endplates and silicone gaskets. A platinum foil (30 mm length, 30 mm width, and 0.22 mm thickness) was used as the counter electrode (CE) and affixed on a polycarbonate endplate. The working electrode (WE), positioned in front of the CE, was fixed to the ABS frame (inside the electrode compartment). The reference electrode, Ag/AgCl (3 M KCl) was inserted into the ABS frame, and positioned to one side towards the top margin of the WE. The blue arrow indicates the electrolyte flow direction. The electrolyte was circulated with a peristaltic pump through the cell (Fig. 1b).

The embroidery WE design (Fig. 2a) consisted of a 24-loop serpentine pattern of about 30 mm length and width. The WEs were oriented with the Cu wires parallel (Fig. 2b), and perpendicular to the electrolyte flow (Fig. 2c). The distance between the Cu lines (about 1.1 mm) was designed to ensure the accessibility of the electrolyte. The Cu wires (80 µm diameter) were embroidered with a 350 dtex polyamide 6.6 (PA6.6) yarn on a nonwoven polypropylene (PP) fabric (Fig. 2d). All constructed electrodes had the same total electrode surface area (1.96 cm^2), which agreed with the electrochemically active surface area as shown in Fig. S1 Supplementary Information. The experiments were conducted in a flow-by configuration (where the electric field is perpendicular to the electrolyte flow and natural convection is neglected), and the area of the CE (9 cm^2) was greater than that of the WE to ensure that the kinetics of the reaction was not limited by the CE.

The 3D-printed ABS flow-distributor frame consists of a matrix of 2 mm cubes separated by a 2 mm distance, to ensure a uniform distribution of the electrolyte flow across the electrode surface (Fig. 3a). MATLAB FEATool Multiphysics was used to solve the incompressible Navier-Stokes 2D equation to estimate the electrolyte velocity distribution for a similar geometry. The boundary conditions used were a no-slip stationary wall, atmospheric outlet pressure, and an arbitrary initial velocity of 10 m s^{-1}. From the resulting 2D electrolyte velocity distribution (Fig. 3b), a laminar flow is expected, and therefore a constant velocity across the electrode compartment. The electrolyte velocity across the cell thickness of 6 mm was considered constant (2D flow field solution in Fig. S2 Supplementary Information).

The composition of the Fe(III)-TEA electrolyte (pH 12.88) was: 0.02 M iron(III) chloride hexahydrate ($FeCl_3{\cdot}6H_2O$, analytical grade, ≥98% p.a., Sigma-Aldrich, Steinheim, Germany), 0.3 M triethanolamine (TEA, technical grade, 85 wt% content in water, Deuring, Hörbranz, Austria), 0.9 M sodium hydroxide (NaOH, analytical grade, ≥99% p.a., Roth, Karlsruhe, Germany). The electrolyte conductivity was about 80 mS cm^{-1} at 26.0 °C (no temperature compensation).

Linear sweep voltammetry curves for the reduction of Fe(III)-TEA were measured from −0.7 V to −1.25 V at a potential sweep rate of 1 mV s^{-1} and at flow rates from 0 to 28.6 mL min^{-1}. The experiments were performed on a VSP Bio-Logics Instruments employing a three-electrode configuration. Negative currents correspond to cathodic reactions (reduction). The electrolyte velocity at each flow rate was calculated by dividing the length distance of the electrode compartment (30 mm) by the time required for the electrolyte to travel this distance. The electrolyte volume in the reservoir was 80 mL, and the volume of the WE compartment was 5.4 mL (30 mm × 30 mm × 6 mm), both considerably larger than the volume of the oxidized electrolyte (Fe(II)-TEA). The redox potential of the reservoir solution was monitored with a RE following the procedure described previously [14], to ensure that the state-of-charge (SOC) remained unchanged through the

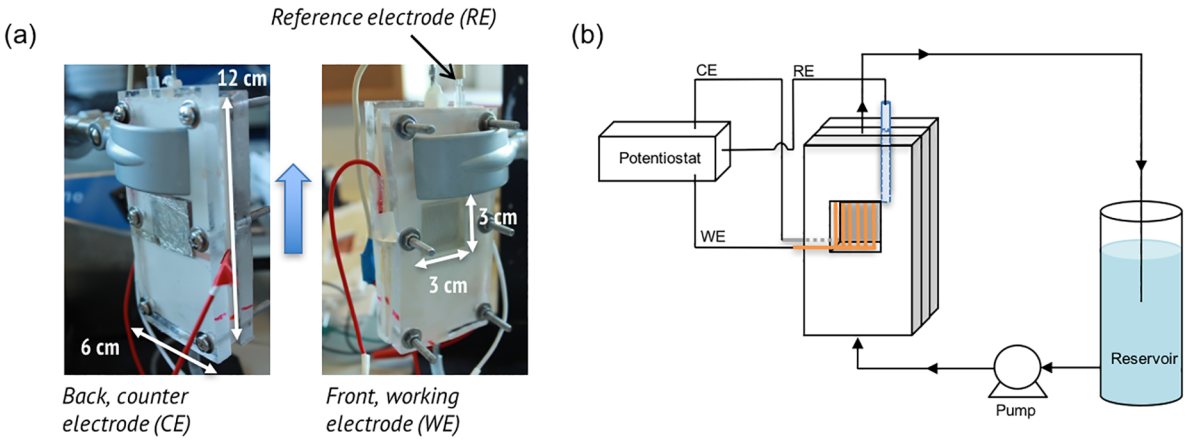

Fig. 1. (a) Constructed flow half-cell consisted of an embroidered Cu electrode as WE, a Pt foil as CE, and a Ag/AgCl (3 M KCl) as RE. A 3D-printed flow-distributor frame (120 mm length, 60 mm width, and 6 mm thickness) was mounted between two polycarbonate endplates. Electrode compartment dimensions of 30 mm length, 30 mm width, and 6 mm thickness (5.4 mL). The blue arrow indicates the electrolyte flow direction. (b) Schematic drawing of the electrolyte flow circuit and electrical connections. (For interpretation of the references to colour in this figure legend, the reader is referred to the web version of this article.)

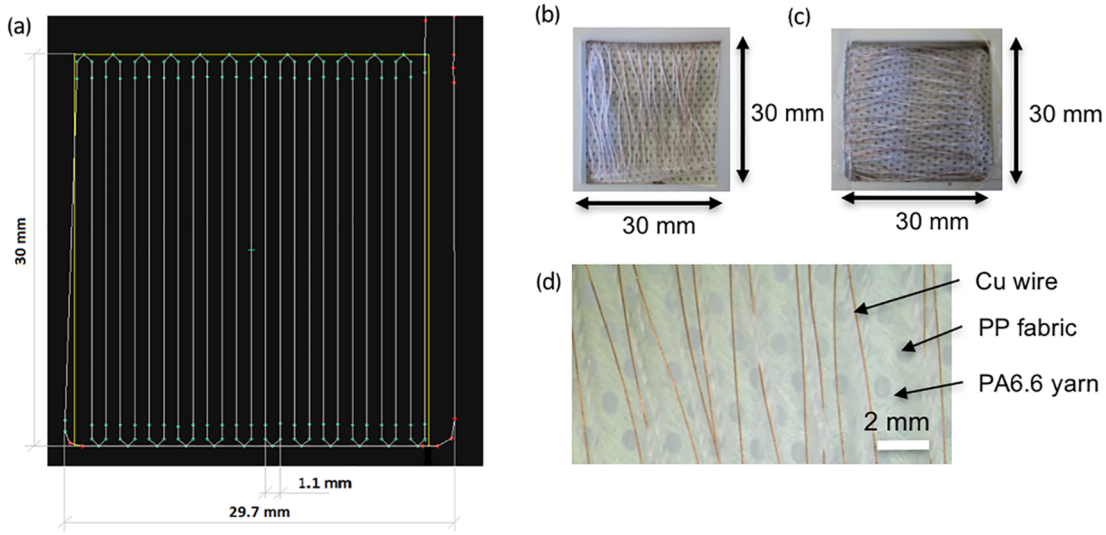

Fig. 2. (a) Embroidered design of the WE. Pictures of the WEs with the two orientations under investigation: (b) parallel, and (c) perpendicular to the electrolyte flow. (d) Photomicrograph of the WE.

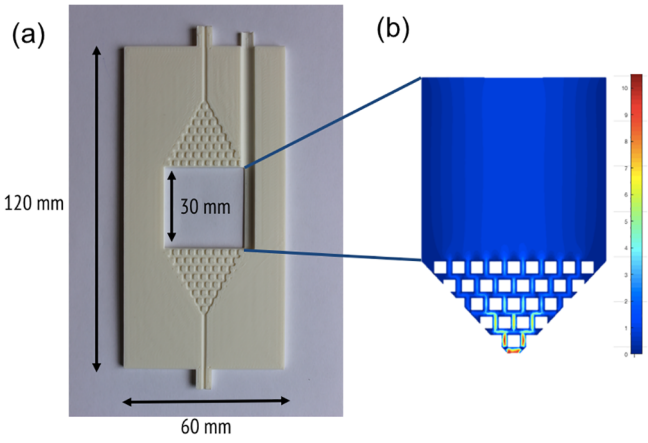

Fig. 3. (a) Front-view picture (half-cut) of the 3D-printed ABS flow-distributor frame. (b) 2D flow field solution of the incompressible Navier-Stokes equation for a similar geometry.

experiments. The oxidation reactions occurring at the CE can be ignored, since the amount of reactant is much larger than the product. The reservoir solution was initially purged with argon, and a blanket of argon was kept over the solution.

3. Results and discussion

The linear sweep voltammetry curves are shown in Fig. 4a. A plateau is observed at greater potentials, which is indicative of the limiting current when the reduction reaction is mass transport controlled. A shift towards negative potentials was observed between the results from perpendicular and parallel Cu wire orientations. That is attributed to potential variations due to drifts in the RE position with respect to the WE that may cause some interferences with the electric field. Evidence for this is observed in the voltammetry curves shown in Fig. S3 (Supplementary Information). Replicate measurements show small deviations in the redox potential, but exhibit the same limiting currents, which is an indicator of potential variations due to the RE position and not other reasons, such as faradaic responses from supporting electrolyte impurities. Such potential differences do not invalidate the results.

The data in Fig. 4a shows that under no flow, where the mass transport is diffusion controlled, both electrode orientations yielded the same limiting currents, which is indicative of no differences in the diffusion layer thickness. That is to be expected since all electrodes had the same Cu wire diameter and the same electroactive surface area. But under flow, the perpendicular orientation yielded higher limiting currents (I_L) than the parallel orientation.

The mass transfer coefficient from each electrode orientation was calculated from the I_L values with Eq. (1):

$$k_m = \frac{I_L}{nFC_BA} \tag{1}$$

where $n = 1$ is the number of electrons involved, F the Faraday constant, A the electrode area, and C_B the bulk Fe(III)-TEA concentration.

The log-log correlation between the calculated mass transfer coefficient and the electrolyte velocity is shown in Fig. 4b. The electrolyte velocity was assumed to be constant across the electrode area. The values followed the well-known empirical equation $k_m = au^b$, with a coefficient of determination, $R^2 = 0.997$ and $R^2 = 0.98$ for the perpendicular and parallel orientations, respectively. The value of exponent b for both orientations was *0.39*, which is in agreement with values found in the literature for heat transfer on single wires (0.385) and mass transport on carbon single fibers (0.4) [15]. The coefficient a, and thereby the mass transfer coefficient k_m, was 18% larger with the perpendicular as compared to the parallel orientation. The same trend has been observed in heat transfer coefficients of parallel and perpendicular flow directions in heat exchangers [16,17], and also for a cylindrical electrolysis cell, where meshes (cathode) were placed in the annular region between a cylindrical anode and the outer wall perpendicular and horizontal to the flow direction [18].

The empirical equation relating the mass transfer coefficients to mean electrolyte velocities was transformed into the dimensionless entities: Sherwood (Sh) and Reynolds (Re) numbers. The relationships obtained were $Sh = 13.9Re^{0.39}$ and $Sh = 11.8Re^{0.39}$ for the perpendicular and parallel orientations, respectively. The Sherwood ($Sh = k_m d_h D^{-1}$) and Reynolds ($Re = ud_h\rho\eta^{-1}$) numbers were calculated by considering as characteristic length (d_h) the distance between wires (1.1 mm) in analogy with the pore diameter in conventional electrodes, the diffusion coefficient as $D = 4.8{\cdot}10^{-6}$ cm^{2}s^{-1} (obtained from Fig. S4 Supplementary Information), a density ρ of about 1.05 g mL^{-1}, and the viscosity η was assumed to be that of water at room temperature, $0.89{\cdot}10^{-4}$ Pas, because of the low concentrations. The calculated Schmidt number ($Sc = \eta^{-1}D^{-1}$) was about 200, which indicates diluted solutions. The Reynolds numbers for our experiments were between $30 < Re < 350$ with an exponent of 0.39, indicating a laminar flow [19]. The electrolyte velocities were close to the range of

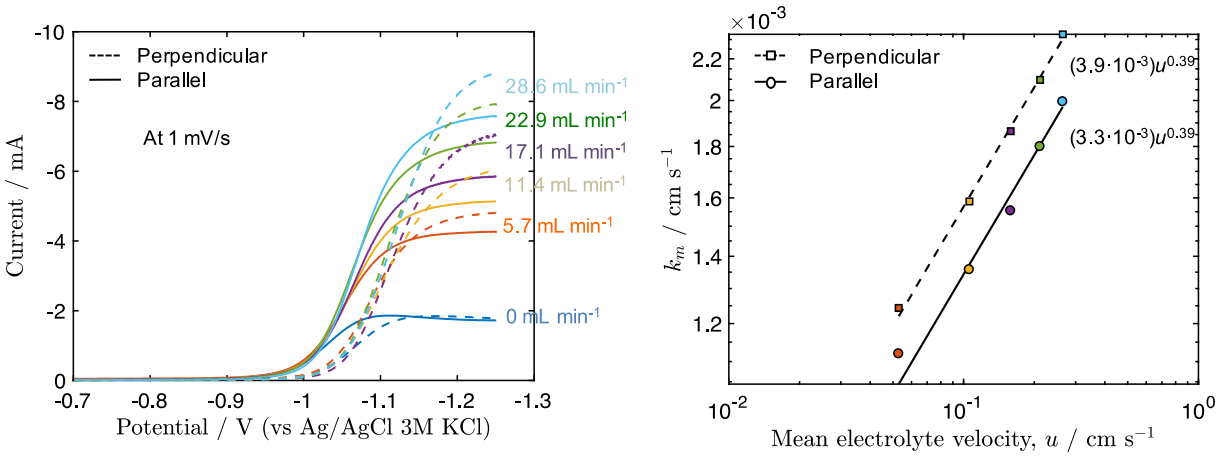

Fig. 4. (a) Linear sweep voltammetry curves at 1 mV s^{-1} and at different volumetric flow rates for Cu wires electrodes oriented perpendicular and parallel to the electrolyte flow. (b) Mass transfer coefficients (k_m) for both electrode orientations with respect to the mean electrolyte velocity.

operational velocities 0.25–1.5 cm s^{-1} in RFBs [8].

The results demonstrated that wires oriented perpendicular to the flow resulted in greater mass transfer coefficients than when wires were oriented parallel to the flow. The results are explained by the greater supply of reactants at the electrode surface for the perpendicular orientation than the horizontal orientation, under our experimental conditions. To provide some insights into the experimental results, we considered the underlying Nernst-Planck theory. Under steady-state conditions (at the limiting current region, where concentration does not change with time) and negligible migration, the general mass-transfer equation can be written as:

$$\frac{\partial C_j}{\partial t} = D\nabla^2 C_j - \vec{u}\cdot\nabla C_j = 0 \tag{2}$$

$$D\left(\frac{\partial^2 C}{\partial z^2} + \frac{\partial^2 C}{\partial x^2}\right) - u\frac{\partial C}{\partial z} = 0 \tag{3}$$

$$D\left(\frac{\partial^2 C}{\partial z^2} + \frac{\partial^2 C}{\partial r^2}\right) + \frac{D}{r}\frac{\partial C}{\partial r} - u\frac{\partial C}{\partial z} = 0 \tag{4}$$

where j represents each specie, D is the diffusion coefficient, and u is the electrolyte velocity. Eq. (3) corresponds to the perpendicular orientation in Cartesian coordinates, and Eq. (4) to the parallel orientation in cylindrical coordinates. Different coordinates were used for symmetry considerations and to maintain the electrolyte velocity always in the z-direction.

The MATLAB FEATool Multiphysics was used to solve the above equations and estimate the 2D concentration profiles of the reduced species for each orientation, when the electrolyte velocity is 0.25 cm s^{-1} (Fig. 5). The boundary conditions used were the following: a complete reduction of the oxidized species at the electrode surface, null concentration of reduced species at the entrance of the electrolyte flow, and outflow condition for the rest of the walls. The condition of artificial isotropic stabilization was used for the perpendicular orientation.

From the concentration profiles, we can observe that the reduced species in the perpendicular orientation are built up on the rearside of the electrode allowing for the reactants free access to the front surface of the electrode. In the parallel orientation, the products accumulate all along the electrode surface, blocking the access to the reactants to the whole electrode surface. This would explain the experimental findings of greater mass transport coefficients for the perpendicular orientation.

It should be noted that our experiments were performed with low specific surface areas and were comprised of a single layer of parallel wires to avoid a non-uniform current distribution across the electrode thickness. We do not expect different findings in conventional RFBs electrodes caused by the difference in the wire and fiber diameters (Cu wires had a diameter of 80 μm, while carbon fibers show 10 μm in diameter). However, the distance between the wires/fibers may have some impact on the observations. In our experiments the space between wires was maintained at 1.1 mm on purpose to enable complete electrolyte accessibility through the electrode and to avoid changes in the state-of-charge. A transfer of the findings obtained with our single-layer wire electrodes to oriented-fiber 3D electrodes indicates that orientation perpendicular to the electrolyte flow promotes mass transfer to the electrodes.

It will also be interesting to perform similar experiments with three-dimensional electrodes of high-packing density constituted of aligned wires/fiber, to measure their impact on electrolyte permeability, and thereby on mass transport. Investigations will be performed in that direction in future work. Some studies have been conducted on that topic, but a clear correlation is not yet defined. As illustration, simulation studies [20] on graphite felts with fibers oriented perpendicular to the flow, showed that it negatively affected the electrolyte permeability and thereby exerted a negative impact on mass transport. With other substrates as carbon cloths, which have about half of the conductive elements oriented perpendicular to the electrolyte flow, a greater mass transport, lower permeability and pressure drop, were observed [11,13].

Another interesting aspect to be considered in fiber orientation is electrolyte infiltration and filling within the electrode. As Tariq and coworkers observed in their studies [21], the electrolyte filling in carbon fiber electrodes is governed by a node-to-node permeation process driven by capillarity. It will be interesting to investigate if this fact may provide a higher permeation in fiber-aligned electrodes, as well as its influence on fiber orientation.

Our findings are limited to the case of a flow-by configuration (electric field perpendicular to the electrolyte flow), and it is not clear that flow-through systems (electric field parallel to the electrolyte flow) will provide the same responses. Previous investigations [22,23] showed that mass transfer coefficients in a flow-by configuration using metal grids and foams electrodes were greater than in a flow-through configuration. To our knowledge, there are no studies comparing both electrode orientations in a flow-through configuration. It will be worthwhile to also to investigate the influence of fiber orientation in this configuration.

4. Conclusions

We investigated the influence of the electrode orientation to the flow direction on the mass transport in a flow-by cell. The flow cell was especially designed via 3D printing to exhibit uniform electrolyte velocity within the electrode. The values obtained for the Reynolds number were in agreement with a laminar flow, for electrolyte velocities close to the values used in redox flow batteries. Greater limiting

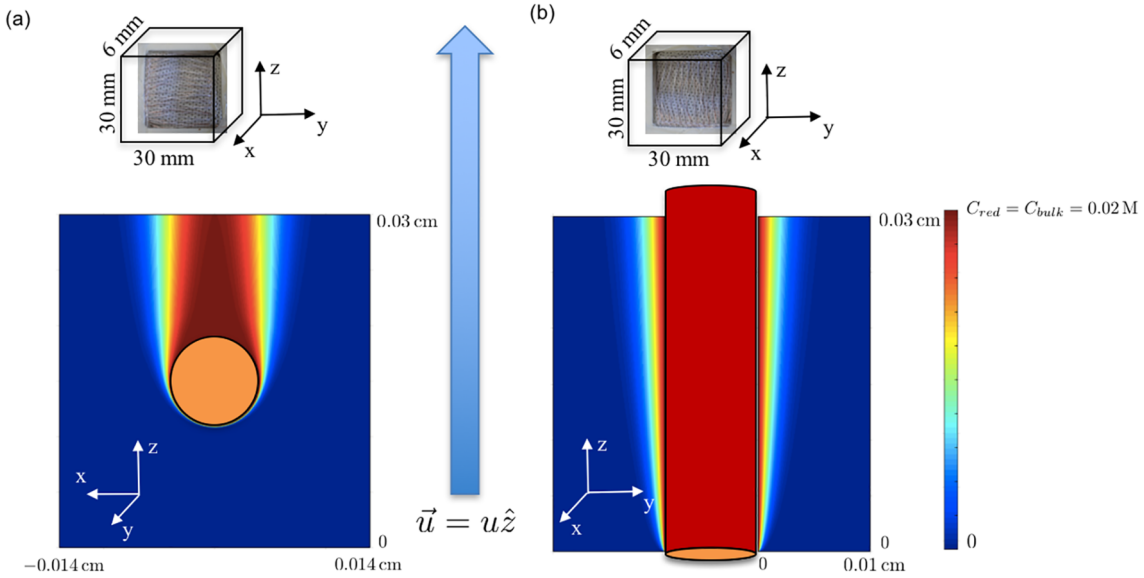

Fig. 5. Steady state concentration profiles of the reduced species (C_{red}) for a single wire in the (a) perpendicular and (b) parallel orientations obtained from the Nernst-Planck equation. The u vector represents the electrolyte velocity. The top images provide a schematic drawing of the electrode compartment.

currents and thus, therefore mass transfer coefficients, were obtained for the electrodes oriented perpendicular to the flow direction. The experiments were performed with wires for a better control of the electrode surface area, but we expect same responses on electrodes composed by carbon fibers. The findings contribute to a greater understanding of the causes of the superior electrochemical performance of fiber-oriented electrodes, such as carbon cloths, in RFBs. The results provide some insights for the optimization of electrodes in mass-transport-limited reactors.

CRediT authorship contribution statement

Noemí Aguiló-Aguayo: Conceptualization, Investigation, Formal analysis, Funding acquisition, Writing - original draft. **Thomas Drozdzik:** Investigation. **Thomas Bechtold:** Supervision, Funding acquisition, Writing - review & editing.

Declaration of Competing Interest

The authors declare that they have no known competing financial interests or personal relationships that could have appeared to influence the work reported in this paper.

Acknowledgments

Author N.A.A. thanks the Austrian Science Fund (FWF) for the Project Embelred T-1041 funded under the Hertha Firnberg Programme, and Dr. Avinash P. Manian and Philipp Schröder for discussions. Authors also acknowledge the K-Project TCCV Nr. 860474 funded by Federal Ministry for Transport, Innovation and Technology (BMVIT), Austrian Federal Ministry of Science, Research and Economy (BMWFW), Land Vorarlberg, Tirol, and Wien within the framework of COMET Competence Centers for Excellence Technologies managed by the Austrian Research Promotion Agency (FFG).

Appendix A. Supplementary data

Supplementary data to this article can be found online at https://doi.org/10.1016/j.elecom.2019.106650.

References

[1] A.Z. Weber, M.M. Mench, J.P. Meyers, P.N. Ross, J.T. Gostick, Q. Liu, J. Appl. Electrochem. 41 (2011) 1137–1164, https://doi.org/10.1007/s10800-011-0348-2.
[2] B.K. Chakrabarti, N.P. Brandon, S.A. Hajimolana, F. Tariq, V. Yufit, M.A. Hashim, et al., J. Power Sources 253 (2014) 150–166, https://doi.org/10.1016/j.jpowsour.2013.12.038.
[3] D.S. Aaron, Q. Liu, Z. Tang, G.M. Grim, A.B. Papandrew, A. Turhan, et al., J. Power Sources 206 (2012) 450–453, https://doi.org/10.1016/j.jpowsour.2011.12.026.
[4] J. Houser, J. Clement, A. Pezeshki, M.M. Mench, J. Power Sources 302 (2016) 369–377, https://doi.org/10.1016/j.jpowsour.2015.09.095.
[5] J.T. Clement, D.S. Aaron, M.M. Mench, J. Electrochem. Soc. 163 (2016) A5220–A5228, https://doi.org/10.1149/2.029305jes.
[6] K.M. Lisboa, R.M. Cotta, Int. J. Heat Mass Transf. 122 (2018) 954–966, https://doi.org/10.1016/j.ijheatmasstransfer.2018.02.002.
[7] X. You, Q. Ye, P. Cheng, ECS Trans. (2016), https://doi.org/10.1149/07208.0187ecst.
[8] X. You, Q. Ye, P. Cheng, J. Electrochem. Soc. 164 (2017) E3386–E3394, https://doi.org/10.1149/2.0401711jes.
[9] J.D. Milshtein, K.M. Tenny, J.L. Barton, J. Drake, R.M. Darling, F.R. Brushett, J. Electrochem. Soc. 164 (2017) E3265–E3275, https://doi.org/10.1149/2.0201711jes.
[10] M.D.R. Kok, R. Jervis, T.G. Tranter, M.A. Sadeghi, D.J.L. Brett, P.R. Shearing, et al., Chem. Eng. Sci. 196 (2019) 104–115, https://doi.org/10.1016/j.ces.2018.10.049.
[11] X.L. Zhou, T.S. Zhao, Y.K. Zeng, L. An, L. Wei, J. Power Sources 329 (2016) 247–254, https://doi.org/10.1016/j.jpowsour.2016.08.085.
[12] X.L. Zhou, T.S. Zhao, L. An, Y.K. Zeng, L. Wei, J. Power Sources 339 (2017) 1–12, https://doi.org/10.1016/j.jpowsour.2016.11.040.
[13] A. Forner-Cuenca, E.E. Penn, A.M. Oliveira, F.R. Brushett, J. Electrochem. Soc. 166 (2019) A2230–A2241, https://doi.org/10.1149/2.0611910jes.
[14] N. Aguiló-Aguayo, T. Bechtold, J. Electrochem. Soc. 165 (2018) A3164–A3168, https://doi.org/10.1149/2.0911813jes.
[15] D. Schmal, J. Van Erkel, P.J. Van Duin, J. Appl. Electrochem. 16 (1986) 422–430, https://doi.org/10.1007/BF01008853.
[16] A.V. Bulgakov, V.G. Prikhod'ko, J. Appl. Mech. Tech. Phys. (1986). doi:10.1007/BF00916150.
[17] T. Samana, T. Kiatsiriroat, A. Nuntaphan, Heat Transf. Eng. 33 (2012) 1033–1039, https://doi.org/10.1080/01457632.2012.659624.
[18] R. Alkire, P.K. Ng, J. Electrochem. Soc. 124 (1977) 1220–1227, https://doi.org/10.1149/1.2133531.
[19] C. Ponce de León, W. Hussey, F. Frazao, D. Jones, E. Ruggeri, Chem. Eng. Trans. 41 (2014) 1–6, https://doi.org/10.3303/CET1441001.
[20] D. Maggiolo, F. Picano, M. Guarnieri, Phys. Fluids 28 (2016), https://doi.org/10.1063/1.4963766.
[21] F. Tariq, J. Rubio-Garcia, V. Yufit, A. Bertei, B.K. Chakrabarti, A. Kucernak, et al., Sustain. Energy Fuels 2 (2018) 2068–2080, https://doi.org/10.1039/c8se00174j.
[22] S. Piovano, U. Böhm, J. Appl. Electrochem. (1987), https://doi.org/10.1007/BF01009138.
[23] S. Langlois, F. Coeuret, J. Appl. Electrochem. 19 (1989) 51–60, https://doi.org/10.1007/BF01039389.